MicroRNA let-7 and miR-278 regulate insect metamorphosis and oogenesis via targeting juvenile hormone early response gene *Krüppel-homolog 1*

Jiasheng Song, Wanwan Li, Haihong Zhao, Lulu Gao, Yuning Fan, Shutang Zhou*

Key Laboratory of Plant Stress Biology, State Key Laboratory of Cotton Biology, School of Life Sciences, Henan University, Kaifeng 475004, China

* Corresponding author:

Shutang Zhou, PhD, Professor

Email: szhou@henu.edu.cn

Summary statement

MicroRNA let-7 and miR-278 are suppressed by juvenile hormone and downregulate the early juvenile hormone-response gene, *Krüppel-homolog 1*. This regulatory loop controls insect metamorphosis and female reproduction.

Key words: microRNA, Kr-h1, juvenile hormone, metamorphosis, female reproduction

ABSTRACT

Krüppel-homolog 1 (Kr-h1), a zinc finger transcription factor, transduces juvenile hormone (JH) signaling in inhibiting larval metamorphosis and promoting adult reproduction. While the transcriptional regulation of *Kr-h1* has been extensively studied, little is known about its regulation at the post-transcriptional level. By using the migratory locust, *Locusta migratoria* as a model system, we report here that microRNA let-7 and miR-278 bound to *Kr-h1* coding sequence and downregulated its expression. Application of let-7 and miR-278 agomiRs significantly reduced the level of *Kr-h1* transcripts, resulting in partially precocious metamorphosis in nymphs as well as markedly decreased yolk protein precursors, arrested ovarian development and blocked oocyte maturation in adults. Moreover, the expression of let-7 and miR-278 was repressed by JH, constituting a regulatory loop of JH signaling. This study thus discovers a previously unknown mechanism by which JH suppresses the expression of let-7 and miR-278, which, together with JH induction on *Kr-h1* transcription, prevents the precocious metamorphosis of nymphs and stimulates the reproduction of adult females. The results advance our understanding in the coordination of JH and miRNA regulation in insect development.

INTRODUCTION

Insect development, metamorphosis and reproduction are primarily controlled by juvenile hormone (JH) and 20-hydroxyecdysone (20E). While 20E initiates larval/ nymphal molting and metamorphosis, JH maintains the juvenile status by repressing the metamorphic action of 20E (Jindra et al., 2015a; Jindra et al., 2013; Riddiford, 1994). JH also stimulates aspects of female reproduction including previtellogenic development, vitellogenesis and oogenesis in many insect species (Raikhel et al., 2005; Roy et al., 2018; Wyatt and Davey, 1996). The molecular action of JH relies on its intracellular receptor Methoprene-tolerant (Met), a member of basic helix-loop-helix Per-Arnt-Sim (bHLH-PAS) transcription factor family (Charles et al., 2011; Jindra et al., 2015b; Li et al., 2011). JH induces the heterodimerization of Met with another bHLH-PAS protein Taiman (Tai) to form an active JH-receptor complex to regulate the transcription of JH-responsive genes (Guo et al., 2014; Kayukawa et al., 2012; Li et al., 2011; Luo et al., 2017; Wu et al., 2018b). Krüppel-homolog 1 (Kr-h1), a C_2H_2 zinc-finger type transcription factor, is a key player in JH signaling pathway. JH-induced Met/Tai complex binds to the JH response element in the promoter of *Kr-h1* and directly activates its transcription (Cui et al., 2014; Kayukawa et al., 2012; Li et al., 2014; Lozano et al., 2014; Shin et al., 2012; Song et al., 2014). In the larval stage, Kr-h1 transduces the anti-metamorphic action of JH in both holometabolous and hemimetabolous insects (Konopova et al., 2011; Lozano and Belles, 2011; Minakuchi et al., 2009; Minakuchi et al., 2008). Kr-h1 prevents immature larvae from initiating precocious larval-pupal transition by repressing the expression of the pupal specifier

gene *Broad-complex* (*BR-C*) (Jindra et al., 2013). Kr-h1 also inhibits precocious adult metamorphosis by suppressing the expression of the adult specifier gene *Ecdysone induced protein 93F* (*E93*) (Belles and Santos, 2014). Recent studies have demonstrated that Kr-h1 binds to the consensus Kr-h1 binding site (KBS) in the promotor regions of *BR-C* and *E93* to directly suppress their transcription (Kayukawa et al., 2017; Kayukawa et al., 2016). Moreover, Kr-h1 can function as an antagonist of 20E synthesis by directly inhibiting the transcription of genes coding for steroidogenic enzymes in prothoracic glands of the fruit fly *Drosophila melanogaster* and the silkworm *Bombyx mori* (Liu et al., 2018; Zhang et al., 2018). The role of Kr-h1 in JH-regulated female reproduction appears to vary amongst insect species. In the mosquito *Aedes aegypti*, Kr-h1 can activate and repress the expression of its target genes for previtellogenic development and egg production in response to JH (Ojani et al., 2018; Shin et al., 2012; Zou et al., 2013). Depletion of *Kr-h1* in adult females of the common bed bug *Cimex lectularius* does not reduce the egg number but severely reduces the egg hatchability (Gujar and Palli, 2016). In the migratory locust *Locusta migratoria*, Kr-h1 mediates JH action to promote vitellogenesis, ovarian development and oocyte maturation (Song et al., 2014). While extensive studies have been conducted to elucidate the transcriptional activation of *Kr-h1* and its regulation on target genes, the regulation of microRNA (miRNA) on *Kr-h1* at the post-transcriptional level is less explored.

miRNAs are ~22-nucleotide non-coding RNAs, complementarily binding to the 3'-untranslated region (3'UTR) or the coding sequence (CDS) of target mRNAs to regulate gene expression at the post-transcriptional level (Forman et al., 2008; Ghildiyal

and Zamore, 2009; Rigoutsos, 2009). Previously, only miR-2 has been demonstrated to target *Kr-h1*. In the cockroach *Blattella germanica*, miR-2 eliminates *Kr-h1* transcripts at the final nymphal instar, which, together with the decrease of JH and concomitant reduction of *Kr-h1* transcription, ensures the onset of metamorphosis (Lozano et al., 2015). miRNAs can also interact with 20E pathway to modulate insect metamorphosis and reproduction (Belles, 2017; Belles et al., 2012; Lucas and Raikhel, 2013; Roy et al., 2018). The let-7 cluster including let-7, miR-100 and miR-125 is regulated by 20E, targeting *abrupt* gene and controlling neuromuscular and wing development during the metamorphosis of *D. melanogaster* (Caygill and Johnston, 2008; Chawla and Sokol, 2012). In *B. mori*, let-7 exerts its function in larval-pupal transition by targeting 20E response genes *FTZ-F1* and *E74* (Ling et al., 2014). In vitellogenic adult females of *Ae. aegypti*, 20E-dependent expression of miR-275 is required for blood digestion, and inhibition of miR-275 leads to incomplete egg development (Bryant et al., 2010). Mosquito-specific miR-1890 is also activated by the 20E pathway, which affects ovarian development by targeting the serine protease gene *JHA15* (Lucas et al., 2015). Despite the understanding of miRNA regulation in 20E-triggered insect metamorphosis and reproduction, little is known about the interaction of miRNA with JH signaling pathway in JH-stimulated vitellogenesis and oogenesis.

L. migratoria has been a favorite model for studying the mechanisms of JH-dependent female reproduction, as JH controls the synthesis of its yolk protein precursor Vitellogenin (Vg) synthesis in the fat body, secretion into the hemolymph and uptake by the maturing oocytes (Raikhel et al., 2005; Roy et al., 2018; Wyatt and Davey,

1996). In the present study, we performed high throughput miRNA sequencing and quantification to identify miRNAs involved in JH pathway. We found that let-7 and miR-278 were regulated by JH and targeted *Kr-h1* via binding to its CDS. The expression of let-7 and miR-8 increased at the final nymphal instar, but decreased in both previtellogenic and vitellogenic stages. Injection of let-7 and miR-278 agomiRs led to markedly reduced Vg proteins, blocked oocyte maturation and impaired ovarian growth in adult female locusts as well as moderate phenotypes of precocious metamorphosis in nymphs. This study thus points to a previously unidentified mechanism by which JH-suppressed miRNAs regulate insect metamorphosis and reproduction via targeting an early JH-response gene.

RESULTS

Identification of miRNAs targeting *Kr-h1*

L. migratoria has abundant miRNAs in its genome (Wang et al., 2015). To elucidate the regulatory mechanisms of miRNA in JH-stimulated vitellogenesis and egg production, we performed high throughput sequencing with small RNA libraries derived from the fat body of adult female locusts within 12 h post adult emergence (0 day PAE) as well as those at 2, 4, 6 days PAE. Totally, 483 miRNAs were identified and 335 miRNAs were found with RPKM values > 10. Of these candidate miRNAs, we chose to focus on the conserved miRNAs because of their crucial role in insect development and conservation across insect orders. Among those with RPKM values > 10, a total of 60 conserved miRNAs were identified by similarity search against

miRBase database (Fig. S1A) (Kozomara and Griffiths-Jones, 2014). These conserved miRNAs could be categorized into 5 hierarchical clusters by complete linkage algorithm with the respective read counts (Fig. 1A). Group 1 consisting of 10 miRNAs showed a general increase of expression from 0 to 6 days PAE. The levels of 6 miRNAs (Group 2) were increased at 2-4 days PAE and then declined at 6 days PAE. In Group 3 comprised of 17 miRNAs, most of them were expressed at gradually lower levels from 2 to 6 days PAE. The expression of 10 miRNAs (Group 4) was decreased at 2 days PAE but thereafter elevated at 4-6 days PAE. The levels of 16 miRNAs (Group 5) were lower at 2-4 days PAE and continually dropped on day 6. Based on the cutoff criteria at fold change > 1.5 and $P < 0.05$, the levels of 24, 22 and 25 miRNAs were significantly declined at 2, 4, 6 days PAE, respectively compared to day 0 (Fig. S1B). In the first gonadotrophic cycle, the adult female locusts undergo previtellogenesis from 0 to 4 days PAE and vitellogenesis started at ~5 days PAE under our rearing condition. The above data indicate that most of conserved miRNAs identified from our large-scale small RNA sequencing are expressed at lower levels during the previtellogenic development and vitellogenesis, compared to that on the day of adult ecdysis.

We next predicted the miRNA binding sites of *Kr-h1* (GenBank: KJ425482) mRNA to identify the conserved miRNAs potentially involved in *Kr-h1* regulation. Seven conserved miRNAs were predicted to bind to *Kr-h1* mRNA sequence. The binding sites of let-7, miR-278, miR-423 and miR-296 were in the CDS (Fig. S1C), whereas miR-14, miR-998 and miR-2765 presumably bound to 3'UTR (Fig. S1D). To validate the binding of predicted miRNAs to *Kr-h1* mRNA, we carried out dual-luciferase reporter

assays by co-transfection of miRNA mimics and recombinant pmirGLO vector with ~500 bp DNA fragments containing the predicted miRNA binding sites into HEK293T cells. When let-7 and miR-278 mimics were co-transfected, luciferase activities declined by 57% and 56%, respectively compared to the non-mimic controls (Fig. 1B). However, co-transfection with miR-296, miR-423, miR-14, miR-998 or miR-2765 mimics had no significant effect on the reporter activity (Fig. 1B and 1C). Knowing that let-7 and miR-278 suppressed the *Kr-h1* reporter activity, we mutated the binding sites complementary to the "seed" sequences of let-7 or miR-278 (Fig. S1C) for further dual-luciferase assays. As shown in Fig. 1D and 1E, the capacity of let-7 or miR-278 to inhibit the *Kr-h1* reporter activity was completely blocked when the mutated sequences were employed. These observations suggest that let-7 and miR-278 bind to the CDS of *Kr-h1* to regulate its expression.

let-7 and miR-278 regulate *Kr-h1* expression *in vivo*

To reveal the dynamics of let-7 and miR-278 expression in the first gonadotrophic cycle, qRT-PCR was conducted using small RNAs isolated from the fat body of adult females at 0-8 days PAE. Compared to that at 0 day PAE, the expression levels of let-7 were significantly decreased by ~67% on day 2-8 (Fig. 2A), while miR-278 expression was significantly declined by 63-68% on day 2-4 and further decreased by 77-79% at 6-8 days PAE (Fig. 2B). A fall in the transcript levels of let-7 and miR-278 appeared to opposite with the elevated mRNA levels of *Kr-h1* (Fig. 2A and 2B) (Song et al., 2014). To evaluate the responsiveness of let-7 and miR-278 to JH, qRT-PCR was performed using small RNAs extracted from the fat body of JH-deprived adult females by ablation

of *corpora allata* with ethoxyprecocene treatment for 10 d (Dhadialla et al., 1987; Zhou et al., 2002) as well as those further treated with a potent JH analogue, methoprene for 6-48 h. As shown in Fig. 2C and 2D, chemical allatectomy by ethoxyprecocene treatment resulted in 1.4-fold and 1.5-fold increase of let-7 and miR-278 expression levels, respectively. Further application of methoprene led to 36% reduction of let-7 expression levels at 48 h (Fig. 2C). The levels of miR-278 declined by 31% and 51%, respectively after methoprene treatment for 24 h and 48 h (Fig. 2D). As the miRNA-Ago1 complex is the key component of RNA-induced silence complex (RISC) for post-transcriptional regulation of target genes, we performed RNA immunoprecipitation (RIP) in the fat body using the monoclonal antibody against locust Argonaute 1 (Ago1) (Yang et al., 2014) to determine the interaction of let-7 and miR-278 with *Kr-h1* mRNA *in vivo*. agomiR, the chemically modified miRNA mimic, is widely used for miRNA function study *in vivo*, resembling the overexpression of same miRNA. Injection of agomiR enhances the abundance of this miRNA, though it does not cause the overexpression of endogenous miRNA. When let-7 agomiR was injected, the abundance of precipitated *Kr-h1* mRNA was 4.2-fold higher than the negative control (Fig. 3A). With respect of miR-278, injection of its agomiR led to 3.3-fold increase of precipitated *Kr-h1* mRNA relative to the negative control (Fig. 3A). These data indicate the *in vivo* binding of let-7 and miR-278 to *Kr-h1* mRNA.

We next evaluated the effect of let-7 and miR-278 agomiR treatment on *Kr-h1* transcript and protein levels. qRT-PCR demonstrated that *Kr-h1* transcripts reduced by 61% and 43% in the fat body of adult females injected with let-7 and miR-278 agomiRs,

respectively (Fig. 3B). Western blot and subsequent quantification of band intensity showed that Kr-h1 protein levels declined to 65% and 47%, respectively of its normal levels after let-7 and miR-278 agomiR treatment (Fig. 3C and 3D). Taken together, the above results indicate that *Kr-h1* is downregulated by let-7 and miR-278.

Injection of let-7 and miR-278 agomiRs blocks vitellogenesis and egg production

Since let-7 and miR-278 were found to target *Kr-h1* and express at low levels in the vitellogenic phase, we determined their function in locust vitellogenesis and egg production by agomiR treatment. All phenotypes were examined at 8 days PAE, when *Vg* expression naturally reached the peak and the primary oocytes were maturing. Compared to that of the negative controls, the abundance of let-7 elevated by 76-fold in the fat body of adult females injected with let-7 agomiR (Fig. 4A). After let-7 agomiR treatment, the transcript levels of *Kr-h1* reduced by 73% (Fig. 4B). In *L. migratoria*, two *Vg* genes, *VgA* (GenBank: KF171066) and *VgB* (GenBank: KX709496) are coordinately expressed in a similar pattern (Dhadialla et al., 1987). *VgA* was selected as a representative. In let-7 agomiR-treated fat bodies, *VgA* mRNA levels decreased by 79% (Fig. 4B). Western blot and band intensity quantification demonstrated that injection of let-7 agomiR caused 71% reduction of VgA protein levels in the fat body (Fig. 4C). Application of let-7 agomiR resulted in blocked maturation of primary oocytes and arrested growth of ovaries. Consequently, the primary oocytes and ovaries of let-7 agomiR-treated adult females were markedly smaller than that of the negative controls (Fig. 4D). Statistically, the average length of primary oocytes of let-7 agomiR-

treated locusts was 3.7 mm, significantly smaller than that of negative controls (5.1 mm) (Fig. 4E).

As for miR-278, its abundance increased by 38-fold after injection of miR-278 agomiR (Fig. 5A). The levels of *Kr-h1* transcript dropped by 57% in miR-278 agomiR-treated fat bodies compared to that in the negative controls. As a result, *VgA* mRNA and protein reduced to 25% and 53%, respectively of their normal levels in the fat body (Fig. 5B and 5C). miR-278 agomiR-treated locusts also showed impaired oocyte maturation and ovarian growth (Fig. 5D), with a significantly smaller primary oocytes (3.5 mm) in comparison with the negative controls (5.1 mm) (Fig. 5E). The defective phenotypes of ovarian growth and oocyte maturation caused by let-7 and miR-278 agomiR treatment resembled that resulted from *Kr-h1* RNAi, though at less severe levels (Song et al., 2014). Collectively, the above observations indicate a pivotal role of let-7 and miR-278 in locust female reproduction.

Application of let-7 and miR-278 agomiRs causes partially precocious metamorphosis

Kr-h1 has a dual role in preventing juvenile metamorphosis and promoting adult reproduction. We next investigated the involvement of let-7 and miR-278 in locust metamorphosis. Compared to the early penultimate 4th instar (N4), let-7 expression significantly increased by 2.2-fold in the whole body of middle 5th instar nymph (N5), and slightly but insignificantly declined to 2.0-fold at late N5 (Fig. S2A). The expression levels of miR-278 significantly elevated by 2.4-fold at early N5, then dropped at middle N5, but increased again to 1.7-fold at late N5 (Fig. S2B). The

elevated expression levels of let-7 and miR-278 at the final nymphal instar appeared to opposite with the decreased levels of *Kr-h1* transcript at this stage (Fig. S2C). To explore the role of let-7 and miR-278 in locust metamorphosis, we treated the penultimate 4th instar nymphs with let-7 and miR-278 agomiRs and examined the resulting phenotypes at 5th instar. After their respective agomiR treatment, the abundance of let-7 and miR-278 increased by 16.2-fold and 10.1-fold, respectively compared to the negative controls (Fig. 6A and 6B). Injection of let-7 and miR-278 agomiRs reduced *Kr-h1* transcripts by 48% and 70%, respectively in the whole body at N5 (Fig. 6C). After let-7 agomiR treatment, 25% of N5 nymphs (3 replicates with 16 locusts in each treatment) showed precocious adult-specific color patterns in the pronotum, and 25% of N5 nymphs had the intermediate phenotypes (Fig. 6D). Similar phenotypes of precocious nymphal-adult transition have been previously reported for the hemimetabolous linden bug, *Pyrrhocoris apterus* (Smykal et al., 2014). When miR-278 agomiR was applied, 12.5% of N5 nymphs (3 replicates with 16 locusts in each treatment) showed adult-specific color patterns in the pronotum, while 37.5% of N5 nymphs had the intermediate phenotypes (Fig. 6D). Notably, the phenotypes of precocious metamorphosis resulted from let-7 and miR-278 agomiR treatment were less severe than that of *Kr-h1* knockdown (Fig. S3). Collectively, these observations suggest that let-7 and miR-278 have a modest regulatory role in locust metamorphosis.

DISCUSSION

Regulation of *Kr-h1* by let-7 and miR-278

As an early JH-response gene immediately downstream of JH receptor, *Kr-h1* plays an indispensable role in insect metamorphosis and reproduction (Belles and Santos, 2014; Lozano and Belles, 2011; Ojani et al., 2018; Song et al., 2014; Ureña et al., 2016). The intracellular JH-receptor complex binds to the JH response elements (E-box or E-box-like motif) in the promoter of *Kr-h1* and directly regulates its transcription (Cui et al., 2014; Kayukawa et al., 2012; Li et al., 2011; Shin et al., 2012; Song et al., 2014). In addition, *Kr-h1* is found to be post-transcriptionally regulated by miR-2 via binding to the 3'UTR of *Kr-h1* (Lozano et al., 2015). In the final instar nymphs of *B. germanica*, miR-2 scavenges *Kr-h1* transcripts, crucially contributing to the onset of metamorphosis (Lozano et al., 2015). In the present study, we performed high throughput miRNA sequencing to identify miRNAs potentially regulating *Kr-h1*. Of 7 conserved miRNAs with the predicted binding sites of *Kr-h1* mRNA, let-7 and miR-278 were documented to downregulate *Kr-h1* expression via binding to its CDS. Thus, our data extend the view in *Kr-h1* regulation at the post-transcriptional levels. Interestingly, miR-2 binding site was not predicted in locust *Kr-h1* mRNA sequence by using the algorithms of miRanda, PITA and MicroTar, suggesting the diversity of miRNA and its target gene interaction in various insect species. Nevertheless, we cannot exclude the possible prediction of miR-2 binding sites of *Kr-h1* mRNA by using

other predicting algorithms. It should be noted that TRIzol reagent was used for miRNA extraction in this study. It has been reported that miRNAs with low GC content might be lost during extraction with TRIzol (Kim et al., 2012).

A single miRNA usually has multiple targets, while multiple miRNAs can regulate a single gene (Bonci et al., 2008; Hashimoto et al., 2013). It has been demonstrated that let-7 regulates *abrupt*, *FTZ-F1* and *E74* to modulate molting and metamorphosis in *D. melanogaster* and *B. mori* (Caygill and Johnston, 2008; Ling et al., 2014). miR-278 targets *expanded*, *pyrethroid resistance-related gene* (*CYP6AG11*), and *insulin-related peptide binding protein 2* (*IBP2*) to modulate energy homeostasis, insecticide resistance and immune response in *D. melanogaster*, *B. mori* and the mosquito *Culex pipiens pallens* (Lei et al., 2015; Teleman et al., 2006; Wu et al., 2016). Intriguingly, the expression of let-7 and miR-278 was repressed by JH. Our results suggest that while JH acts through Met/Tai to induce *Kr-h1* transcription, JH also suppresses the expression of let-7 and miR-278 to maintain a proper level of Kr-h1 essential for suppressing precocious nymphal metamorphosis and promoting JH-dependent female reproduction in *L. migratoria*. In hemimetabolous *B. germanica*, JH represses the expression of let-7 that contributes to the formation of wings during metamorphosis, possibly through modulating *BR-C* (Rubio and Belles, 2013; Rubio et al., 2012). In *D. melanogaster*, miR-14 targets *EcR*, whereas 20E represses the expression of miR-14, consequently leading to elevated EcR levels and amplified 20E signaling (Varghese and Cohen, 2007). Similar regulatory loop has also been reported for miR-281, EcR-B and 20E in *B. mori* (Jiang et al., 2013). These regulatory loops may typically represent the

adaption of JH- and 20E-modulated gene regulation during the evolution of insect metamorphosis and reproduction.

let-7 and miR-278 in Kr-h1 mediated insect reproduction and metamorphosis

In a previous report, we have demonstrated that *Kr-h1* knockdown in adult female locusts causes substantial reduction of *Vg* expression as well as blocked oocyte maturation and arrested ovarian growth (Song et al., 2014). In this study, let-7 and miR-278 agomiR treatment caused significant reduction of *Kr-h1* transcripts. Application of let-7 and miR-278 agomiRs also markedly reduced the levels of *Vg* expression, accompanied by inhibited oocyte maturation and impaired ovarian growth. These observations provide the evidence that let-7 and miR-278 are crucial players in JH-dependent locust vitellogenesis and egg production.

We also examined the effect of let-7 and miR-278 agomiR treatment on locust molting, as their target gene, *Kr-h1* plays an essential role in repressing larval-pupal and larval-adult transition (Belles and Santos, 2014; Konopova et al., 2011; Lozano and Belles, 2011; Minakuchi et al., 2009; Minakuchi et al., 2008). Application of let-7 and miR-278 agomiRs in the penultimate instar nymphs caused partially precocious metamorphosis as shown by the presence of adult-specific patterns on the pronotum. Notably, the defective phenotypes of female reproduction and precocious metamorphosis caused by treatment of let-7 or miR-278 agomiRs were less severe than that resulted from *Kr-h1* RNAi, suggesting the fine-tuning by miRNAs. Another possibility might be that some phenotypes are counteracted by other genes targeted by let-7 or miR-278. Moreover, *Kr-h1* transcript levels declined by 48-60% after let-7 and

miR-278 agomiR treatment, whereas up to 92% knockdown efficiency was obtained with *Kr-h1* RNAi. The presence of more *Kr-h1* transcripts in agomiR-treated locusts than *Kr-h1*-depleted individuals might also attribute to these less severe phenotypes.

Based on our findings, we propose that while JH acts thorough its intracellular receptor to induce *Kr-h1* transcription, JH also represses the expression of let-7 and miR-278 to maintain the proper levels of Kr-h1 essential for metamorphosis and reproduction in locusts. At the final nymphal instar, the declined JH titer and increased abundance of let-7 and miR-278 lead to low levels of *Kr-h1* expression, which contributes to the onset of metamorphosis. In the previtellogenic and vitellogenic adult females, the increased JH titer and declined abundance of let-7 and miR-278 ensure high levels of *Kr-h1* expression, consequently stimulating the vitellogenesis and oogenesis.

MATERIALS AND METHODS

Ethics statement

Maintenance of, and experiments on rabbits were approved by Medical and Scientific Research Ethics Committee of Henan University.

Experimental animals

The gregarious phase of migratory locust was reared under a 14L:10D photoperiod and at 30 ± 2 ºC. The diet included a continuous supply of dry wheat bran with fresh wheat seedlings provided twice per day. JH-deprived adult female locusts were obtained by topical application of 500 μg (100 μg/μl dissolved in acetone) ethoxyprecocene

(Sigma-Aldrich) per locust to inactivate the corpora allata within 12 h after adult emergence (Dhadialla et al., 1987; Zhou et al., 2002). To restore JH activity, s-(+)-methoprene (Santa Cruz Biotech) was topically applied at 150 µg (30 µg/µl dissolved in acetone) per locust 10 d post ethoxyprecocene treatment as previously described (Dhadialla et al., 1987; Zhou et al., 2002).

small RNA sequencing and data processing

Small RNA sequencing and quantification were performed with small RNA libraries derived from the fat body of adult females at 0, 2, 4 and 6 days post adult emergence, using the Illumina HiSeq 2500 platform. The clean reads were obtained by eliminating the low-quality reads, empty adapters, reads shorter than 18 nt, and reads with Poly(A) tail. Sequences of tRNA, rRNA, snRNA, snoRNA and piRNA were removed by similarity search using the Rfam12.1 and piRNABank database. miRNAs were identified by blasting the rest sequences with miRBase (V21) and referring to the locust genome (Wang et al., 2014). miRanda (V3.3a) (Enright et al., 2003), PITA (V6) and MicroTar (V0.9.6) (Thadani and Tammi, 2006) were employed for prediction of miRNA binding sites.

RNA extraction and qRT-PCR

Total RNA from the whole body and selected tissues was isolated using TRIzol reagent (Thermo Fisher), and cDNA was reverse transcribed with the FastQuant RT Kit (Tiangen). qRT-PCR was performed using a LightCycler 96 System (Roche) and the SuperReal PreMix Plus kit (Tiangen), initiated at 95ºC for 2 min, followed by 40 cycles

of 95°C for 20 s, 58°C for 20 s, and 68°C for 20 s. For miRNA, cDNA was synthesized from total RNA using miRNA first strand cDNA synthesis kit (Tiangen). qRT-PCR for miRNA was conducted using Roche LightCycler system and miRcute miRNA qPCR kit (Tiangen) at 94 °C for 2 min plus 40 cycles of 94 °C for 20 s and 60 °C for 34 s. The relative expression levels were calculated using the $2^{-\Delta\Delta Ct}$ method, with β-actin and U6 as the internal controls of gene and miRNA, respectively. Primers used for qRT-PCR are listed in Table S1.

Luciferase reporter assay

Kr-h1 cDNA fragments with miRNA binding sites were cloned into pmirGLO vector (Promega) and confirmed by sequencing. For site mutation, the seed regions of let-7 and miR-278 binding sites were mutated to their complementary sequences using Site-directed and Ligase-Independent Mutagenesis (Chiu et al., 2004). The constructed vectors, miRNA mimics or the negative control (GenePharma) were then transfected into HEK293T cells (cells were kindly provided by Stem Cell Bank, Chinese Academy of Sciences) using lipofectamine 3000 (Thermo Fisher). After 36h, the luciferase activity was measured using the Dual-Glo Luciferase Assay System (Promega) and analyzed with GloMax 96 Microplate Luminometer (Promega). Primers used for site mutation are included in Table S1.

RNA immunoprecipitation (RIP)

RIP experiments were performed using Magna RIP Kit (Millipore) according to the manufacture's instruction. Briefly, freshly dissected fat bodies were homogenized

in ice-cold RIP lysis buffer, centrifuged for 15 min at 14,000 ×g, and stored at -80 °C overnight. After further centrifugation for 15 min at 14,000 ×g, the supernatant was incubated at 4 °C for 4 h with magnetic beads pre-incubated with a monoclonal antibody against locust Ago1 (Yang et al., 2014) or normal mouse IgG. The precipitated RNA was eluted and reverse transcribed to cDNA using Superscript IV reverse transcriptase and random hexamers (Thermo Fisher), followed by quantification using qRT-PCR.

RNA interference and agomiR treatment

For RNAi experiments, Kr-h1 and green fluorescent protein (GFP) dsRNAs were synthesized using T7 RiboMAX Express RNAi system (Promega). The 4th instar nymphs and adult females were intra-abdominally injected with 5 μg dsRNA within 24 h post nymphal molting and within 12 h after adult emergence, respectively. For agomiR treatment, 4th instar nymphs within 24 h post molting and adult females within 12 h after adult emergence were intra-abdominally injected with 0.5 nmol and 1 nmol agomiR (GenePharma), respectively mixed with *in vivo* RNA Transfection Reagent (Engreen). The sequence from *Caenorhabditis elegans* genome (sense: 5'-UUC UCC GAA CGU GUC ACG UTT-3'; antisense: 5'- ACG UGA CAC GUU CGG AGA ATT-3') was used as the negative control of agomiR (Sun et al., 2013; Wu et al., 2018a). Treatment of agomiR on adult females was boosted twice on day 3 and day 6.

Kr-h1 antibody preparation

A 756-bp cDNA fragment coding for a 252-aa peptide (forward primer: 5'-CGG GGT ACC TAC AAG TGC GAC GTG TGC GA-3'; reverse primer: 5'-CCG GAA TTC CAG GTA GTA GTA GCA GAG GT-3') of locust *Kr-h1* was cloned into pET-32a-His and confirmed by sequencing. The recombinant Kr-h1 peptide was purified by NTA-Ni2+-affinity column (CWBIO) and examined by SDS-PAGE. Polyclonal antibody against Kr-h1 was raised in rabbits using the Kr-h1 peptide mixed with Freund's complete adjuvant (Sigma-Aldrich) to form a stable emulsion for immunization. The New Zealand White rabbits (*Oryctolagus cuniculus*) were injected subcutaneously at 4 sites and boosted once a week for a total of 4 times. The antiserum specificity was verified by western blot using protein extracts from the fat body treated with dsKr-h1 vs. dsGFP.

Western blot

Total proteins were extracted from the whole body of nymphs or the fat body of adult females using the lysis buffer containing 50 mM Tris-HCl (pH 7.5), 150 mM NaCl, 2 mM EDTA, 1 mM DTT, 1% Triton X-100, 1 mM PMSF and a protease inhibitor cocktail (Roche). The tissue lysates were then cleared by centrifugation at 4 ^{o}C for 30 min. Extracted proteins were quantified using BCA protein assay kit (Pierce), fractionated on 8% SDS-PAGE, and then transferred to PVDF membranes (Millipore) Western blot was carried out using antibodies against locust Kr-h1 (1: 2000) and VgA

(1:5000) (Luo et al., 2017). β-actin was used as a loading control. The corresponding HRP-conjugated secondary antibodies (BOSTER) and enhanced ECL Western Blotting Substrate (BOSTER) were employed for chemiluminescent. Bands were imaged with an Amersham Imager 600 (GE Healthcare) and analyzed using ImageJ software.

Data analysis

Statistical analyses were performed by Student's *t* test or One-way ANOVA with LSD (Least Significant Difference) post hoc tests using the SPSS 21.0 software. Values were shown as mean ± SEM and significant difference was considered at $P < 0.05$.

Competing interests

The authors declare no competing or financial interests.

Author contributions

Conceptualization: J.S., S.Z.; Methodology: J.S., S.Z.; Formal analysis: J.S., S.Z.; Investigation: J.S., W.L., H.Z., L.G., Y.F., S.Z.; Writing: S.Z., J.S.; Funding acquisition: S.Z., J.S.

Funding

This work was supported by National Natural Science Foundation of China (NSFC) grants 31372258, 31702063 and 31630070.

Supplementary information

Supplementary information is available online

References

Belles, X. (2017). MicroRNAs and the Evolution of Insect Metamorphosis. *Annu Rev Entomol* **62**, 111-125.

Belles, X., Cristino, A. S., Piulachs, M.-D., Rubio, M. and Tanaka, E. D. (2012). Insect MicroRNAs: from Molecular Mechanisms to Biological Roles. Elsevier Science B.V.

Belles, X. and Santos, C. G. (2014). The MEKRE93 (Methoprene tolerant-Kruppel homolog 1-E93) pathway in the regulation of insect metamorphosis, and the homology of the pupal stage. *Insect Biochem Mol Biol* **52**, 60-68.

Bonci, D., Coppola, V., Musumeci, M., Addario, A., Giuffrida, R., Memeo, L., D'Urso, L., Pagliuca, A., Biffoni, M., Labbaye, C., et al. (2008). The miR-15a-miR-16-1 cluster controls prostate cancer by targeting multiple oncogenic activities. *Nat Med* **14**, 1271-1277.

Bryant, B., Macdonald, W. and Raikhel, A. S. (2010). microRNA miR-275 is indispensable for blood digestion and egg development in the mosquito *Aedes aegypti*. *Proc Natl Acad Sci U S A* **107**, 22391-22398.

Caygill, E. E. and Johnston, L. A. (2008). Temporal regulation of metamorphic processes in *Drosophila* by the let-7 and miR-125 heterochronic microRNAs. *Curr Biol* **18**, 943-950.

Charles, J. P., Iwema, T., Epa, V. C., Takaki, K., Rynes, J. and Jindra, M. (2011). Ligand-binding properties of a juvenile hormone receptor, Methoprene-tolerant. *Proc Natl Acad Sci U S A* **108**, 21128-21133.

Chawla, G. and Sokol, N. S. (2012). Hormonal activation of let-7-C microRNAs via EcR is required for adult *Drosophila melanogaster* morphology and function. *Development* **139**, 1788-1797.

Chiu, J., March, P. E., Lee, R. and Tillett, D. (2004). Site-directed, Ligase-Independent Mutagenesis (SLIM): a single-tube methodology approaching 100% efficiency in 4 h. *Nucleic Acids Res* **32**, e174.

Cui, Y., Sui, Y., Xu, J., Zhu, F. and Palli, S. R. (2014). Juvenile hormone regulates *Aedes aegypti* Kruppel homolog 1 through a conserved E box motif. *Insect Biochem Mol Biol* **52**, 23-32.

Dhadialla, T. S., Cook, K. E. and Wyatt, G. R. (1987). Vitellogenin mRNA in locust fat body: coordinate induction of two genes by a juvenile hormone analog. *Dev Biol* **123**, 108-114.

Enright, A. J., John, B., Gaul, U., Tuschl, T., Sander, C. and Marks, D. S. (2003). MicroRNA targets in Drosophila. *Genome Biol* **5**, R1.

Forman, J. J., Legesse-Miller, A. and Coller, H. A. (2008). A search for conserved sequences in coding regions reveals that the let-7 microRNA targets Dicer within its coding sequence. *Proc Natl Acad Sci U S A* **105**, 14879-14884.

Ghildiyal, M. and Zamore, P. D. (2009). Small silencing RNAs: an expanding universe. *Nat Rev Genet* **10**, 94-108.

Gujar, H. and Palli, S. R. (2016). Juvenile hormone regulation of female reproduction in the common bed bug, *Cimex lectularius*. *Sci Rep* **6**, 35546.

Guo, W., Wu, Z., Song, J., Jiang, F., Wang, Z., Deng, S., Walker, V. K. and Zhou,

S. (2014). Juvenile hormone-receptor complex acts on mcm4 and mcm7 to promote polyploidy and vitellogenesis in the migratory locust. *PLoS Genet* **10**, e1004702.

Hashimoto, Y., Akiyama, Y. and Yuasa, Y. (2013). Multiple-to-multiple relationships between microRNAs and target genes in gastric cancer. *PLoS One* **8**, e62589.

Jiang, J., Ge, X., Li, Z., Wang, Y., Song, Q., Stanley, D. W., Tan, A. and Huang, Y. (2013). MicroRNA-281 regulates the expression of ecdysone receptor (EcR) isoform B in the silkworm, *Bombyx mori*. *Insect Biochem Mol Biol* **43**, 692-700.

Jindra, M., Belles, X. and Shinoda, T. (2015a). Molecular basis of juvenile hormone signaling. *Curr Opin Insect Sci* **11**, 39-46.

Jindra, M., Palli, S. R. and Riddiford, L. M. (2013). The juvenile hormone signaling pathway in insect development. *Annu Rev Entomol* **58**, 181-204.

Jindra, M., Uhlirova, M., Charles, J. P., Smykal, V. and Hill, R. J. (2015b). Genetic Evidence for Function of the bHLH-PAS Protein Gce/Met As a Juvenile Hormone Receptor. *PLoS Genet* **11**, e1005394.

Kayukawa, T., Jouraku, A., Ito, Y. and Shinoda, T. (2017). Molecular mechanism underlying juvenile hormone-mediated repression of precocious larval-adult metamorphosis. *Proc Natl Acad Sci U S A* **114**, 1057-1062.

Kayukawa, T., Minakuchi, C., Namiki, T., Togawa, T., Yoshiyama, M., Kamimura, M., Mita, K., Imanishi, S., Kiuchi, M., Ishikawa, Y., et al. (2012). Transcriptional regulation of juvenile hormone-mediated induction of Kruppel homolog 1, a repressor of insect metamorphosis. *Proc Natl Acad Sci U S A* **109**, 11729-11734.

Kayukawa, T., Nagamine, K., Ito, Y., Nishita, Y., Ishikawa, Y. and Shinoda, T. (2016). Kruppel Homolog 1 Inhibits Insect Metamorphosis via Direct Transcriptional Repression of Broad-Complex, a Pupal Specifier Gene. *J Biol Chem* **291**, 1751-1762.

Kim, Y. K., Yeo, J., Kim, B., Ha, M. and Kim, V. N. (2012). Short structured RNAs with low GC content are selectively lost during extraction from a small number of cells. *Mol Cell* **46**, 893-895.

Konopova, B., Smykal, V. and Jindra, M. (2011). Common and distinct roles of juvenile hormone signaling genes in metamorphosis of holometabolous and hemimetabolous insects. *PLoS One* **6**, e28728.

Kozomara, A. and Griffiths-Jones, S. (2014). miRBase: annotating high confidence microRNAs using deep sequencing data. *Nucleic Acids Res* **42**, D68-73.

Lei, Z., Lv, Y., Wang, W., Guo, Q., Zou, F., Hu, S., Fang, F., Tian, M., Liu, B., Liu, X., et al. (2015). MiR-278-3p regulates pyrethroid resistance in *Culex pipiens pallens*. *Parasitol Res* **114**, 699-706.

Li, M., Liu, P., Wiley, J. D., Ojani, R., Bevan, D. R., Li, J. and Zhu, J. (2014). A steroid receptor coactivator acts as the DNA-binding partner of the methoprene-tolerant protein in regulating juvenile hormone response genes. *Mol Cell Endocrinol* **394**, 47-58.

Li, M., Mead, E. A. and Zhu, J. (2011). Heterodimer of two bHLH-PAS proteins mediates juvenile hormone-induced gene expression. *Proc Natl Acad Sci U S A*

108, 638-643.

Ling, L., Ge, X., Li, Z., Zeng, B., Xu, J., Aslam, A. F., Song, Q., Shang, P., Huang, Y. and Tan, A. (2014). MicroRNA Let-7 regulates molting and metamorphosis in the silkworm, *Bombyx mori*. *Insect Biochem Mol Biol* **53**, 13-21.

Liu, S., Li, K., Gao, Y., Liu, X., Chen, W., Ge, W., Feng, Q., Palli, S. R. and Li, S. (2018). Antagonistic actions of juvenile hormone and 20-hydroxyecdysone within the ring gland determine developmental transitions in *Drosophila*. *Proc Natl Acad Sci U S A* **115**, 139-144.

Lozano, J. and Belles, X. (2011). Conserved repressive function of Kruppel homolog 1 on insect metamorphosis in hemimetabolous and holometabolous species. *Sci Rep* **1**, 163.

Lozano, J., Kayukawa, T., Shinoda, T. and Belles, X. (2014). A role for Taiman in insect metamorphosis. *PLoS Genet* **10**, e1004769.

Lozano, J., Montanez, R. and Belles, X. (2015). MiR-2 family regulates insect metamorphosis by controlling the juvenile hormone signaling pathway. *Proc Natl Acad Sci U S A* **112**, 3740-3745.

Lucas, K. and Raikhel, A. S. (2013). Insect microRNAs: biogenesis, expression profiling and biological functions. *Insect Biochem Mol Biol* **43**, 24-38.

Lucas, K. J., Zhao, B., Roy, S., Gervaise, A. L. and Raikhel, A. S. (2015). Mosquito-specific microRNA-1890 targets the juvenile hormone-regulated serine protease JHA15 in the female mosquito gut. *RNA Biol* **12**, 1383-1390.

Luo, M., Li, D., Wang, Z., Guo, W., Kang, L. and Zhou, S. (2017). Juvenile hormone differentially regulates two Grp78 genes encoding protein chaperones required for insect fat body cell homeostasis and vitellogenesis. *J Biol Chem* **292**, 8823-8834.

Minakuchi, C., Namiki, T. and Shinoda, T. (2009). Kruppel homolog 1, an early juvenile hormone-response gene downstream of Methoprene-tolerant, mediates its anti-metamorphic action in the red flour beetle *Tribolium castaneum*. *Dev Biol* **325**, 341-350.

Minakuchi, C., Zhou, X. and Riddiford, L. M. (2008). Kruppel homolog 1 (Kr-h1) mediates juvenile hormone action during metamorphosis of *Drosophila melanogaster*. *Mech Dev* **125**, 91-105.

Ojani, R., Fu, X., Ahmed, T., Liu, P. and Zhu, J. (2018). Kruppel homologue 1 acts as a repressor and an activator in the transcriptional response to juvenile hormone in adult mosquitoes. *Insect Mol Biol* **27**, 268-278.

Raikhel, A. S., Brown, M. R. and Belles, X. (2005). Hormonal Control of Reproductive Processes. In *Comprehensive Molecular Insect Science* (ed. L. I. Gilbert), pp. 433-491. Amsterdam: Elsevier.

Riddiford, L. M. (1994). Cellular and Molecular Actions of Juvenile-Hormone .1. General-Considerations and Premetamorphic Actions. *Adv Insect Physiol, Vol 24* **24**, 213-274.

Rigoutsos, I. (2009). New tricks for animal microRNAS: targeting of amino acid coding regions at conserved and nonconserved sites. *Cancer Res* **69**, 3245-3248.

Roy, S., Saha, T. T., Zou, Z. and Raikhel, A. S. (2018). Regulatory Pathways

Controlling Female Insect Reproduction. *Annu Rev Entomol* **63**, 489-511.

Rubio, M. and Belles, X. (2013). Subtle roles of microRNAs let-7, miR-100 and miR-125 on wing morphogenesis in hemimetabolan metamorphosis. *J Insect Physiol* **59**, 1089-1094.

Rubio, M., de Horna, A. and Belles, X. (2012). MicroRNAs in metamorphic and non-metamorphic transitions in hemimetabolan insect metamorphosis. *BMC Genomics* **13**, 386.

Shin, S. W., Zou, Z., Saha, T. T. and Raikhel, A. S. (2012). bHLH-PAS heterodimer of methoprene-tolerant and Cycle mediates circadian expression of juvenile hormone-induced mosquito genes. *Proc Natl Acad Sci U S A* **109**, 16576-16581.

Smykal, V., Daimon, T., Kayukawa, T., Takaki, K., Shinoda, T. and Jindra, M. (2014). Importance of juvenile hormone signaling arises with competence of insect larvae to metamorphose. *Dev Biol* **390**, 221-230.

Song, J., Wu, Z., Wang, Z., Deng, S. and Zhou, S. (2014). Kruppel-homolog 1 mediates juvenile hormone action to promote vitellogenesis and oocyte maturation in the migratory locust. *Insect Biochem Mol Biol* **52**, 94-101.

Sun, Y., Li, Q., Gui, H., Xu, D. P., Yang, Y. L., Su, D. F. and Liu, X. (2013). MicroRNA-124 mediates the cholinergic anti-inflammatory action through inhibiting the production of pro-inflammatory cytokines. *Cell Res* **23**, 1270-1283.

Teleman, A. A., Maitra, S. and Cohen, S. M. (2006). *Drosophila* lacking microRNA miR-278 are defective in energy homeostasis. *Genes Dev* **20**, 417-422.

Thadani, R. and Tammi, M. T. (2006). MicroTar: predicting microRNA targets from RNA duplexes. *BMC Bioinformatics* **7 Suppl 5**, S20.

Ureña, E., Chafino, S., Manjon, C., Franch-Marro, X. and Martin, D. (2016). The Occurrence of the Holometabolous Pupal Stage Requires the Interaction between E93, Kruppel-Homolog 1 and Broad-Complex. *PLoS Genet* **12**, e1006020.

Varghese, J. and Cohen, S. M. (2007). microRNA miR-14 acts to modulate a positive autoregulatory loop controlling steroid hormone signaling in *Drosophila*. *Genes Dev* **21**, 2277-2282.

Wang, X., Fang, X., Yang, P., Jiang, X., Jiang, F., Zhao, D., Li, B., Cui, F., Wei, J., Ma, C., et al. (2014). The locust genome provides insight into swarm formation and long-distance flight. *Nat Commun* **5**, 2957.

Wang, Y., Jiang, F., Wang, H., Song, T., Wei, Y., Yang, M., Zhang, J. and Kang, L. (2015). Evidence for the expression of abundant microRNAs in the locust genome. *Sci Rep* **5**, 13608.

Wu, P., Qin, G., Qian, H., Chen, T. and Guo, X. (2016). Roles of miR-278-3p in IBP2 regulation and *Bombyx mori* cytoplasmic polyhedrosis virus replication. *Gene* **575**, 264-269.

Wu, Y., Li, X., Jia, J., Zhang, Y., Li, J., Zhu, Z., Wang, H., Tang, J. and Hu, J. (2018a). Transmembrane E3 ligase RNF183 mediates ER stress-induced apoptosis by degrading Bcl-xL. *Proc Natl Acad Sci U S A* **115**, E2762-e2771.

Wu, Z., Guo, W., Yang, L., He, Q. and Zhou, S. (2018b). Juvenile hormone promotes

locust fat body cell polyploidization and vitellogenesis by activating the transcription of Cdk6 and E2f1. *Insect Biochem Mol Biol* **102**, 1-10.

Wyatt, G. R. and Davey, K. G. (1996). Cellular and molecular actions of juvenile hormone. II. Roles of juvenile hormone in adult insects. *Adv Insect Physiol, Vol 26* **26**, 1-155.

Yang, M., Wei, Y., Jiang, F., Wang, Y., Guo, X., He, J. and Kang, L. (2014). MicroRNA-133 inhibits behavioral aggregation by controlling dopamine synthesis in locusts. *PLoS Genet* **10**, e1004206.

Zhang, T., Song, W., Li, Z., Qian, W., Wei, L., Yang, Y., Wang, W., Zhou, X., Meng, M., Peng, J., et al. (2018). Kruppel homolog 1 represses insect ecdysone biosynthesis by directly inhibiting the transcription of steroidogenic enzymes. *Proc Natl Acad Sci U S A* **115**, 3960-3965.

Zhou, S., Zhang, J., Hirai, M., Chinzei, Y., Kayser, H., Wyatt, G. R. and Walker, V. K. (2002). A locust DNA-binding protein involved in gene regulation by juvenile hormone. *Mol Cell Endocrinol* **190**, 177-185.

Zou, Z., Saha, T. T., Roy, S., Shin, S. W., Backman, T. W., Girke, T., White, K. P. and Raikhel, A. S. (2013). Juvenile hormone and its receptor, methoprene-tolerant, control the dynamics of mosquito gene expression. *Proc Natl Acad Sci U S A* **110**, E2173-2181.

Figures

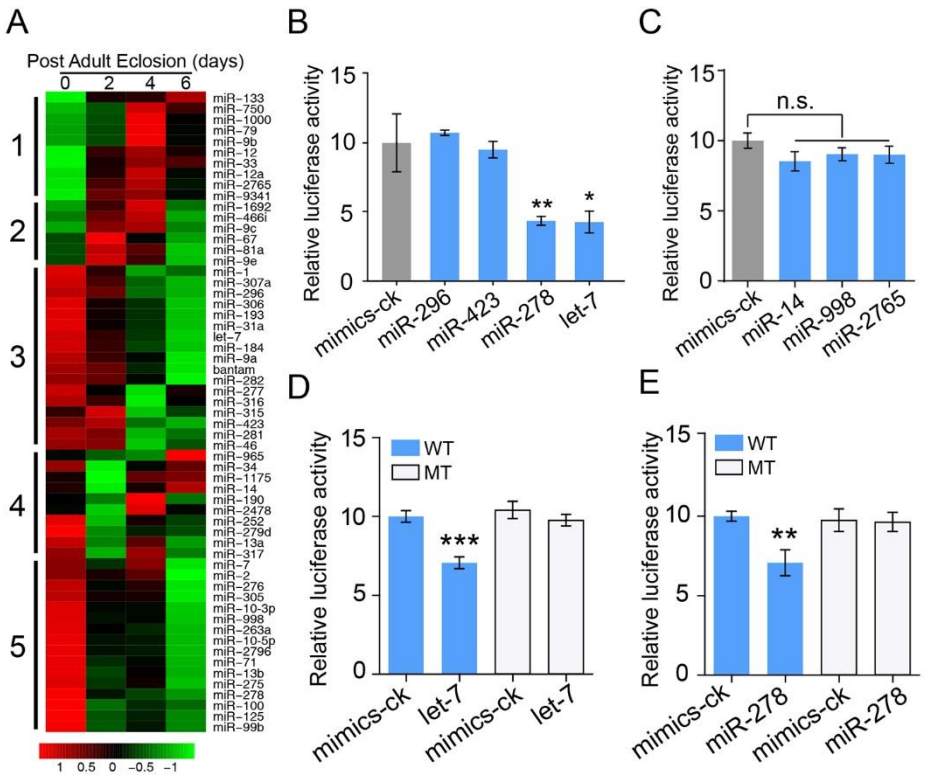

Fig. 1. Identification of miRNAs potentially targeting *Kr-h1*. (A) Heatmap indicating the temporal expression patterns of 60 conserved miRNA identified from small RNA sequencing and quantification of fat bodies collected from adult female locusts at 0, 2, 4 and 6 days post adult eclosion. Numbers at the left indicate the classified groups of miRNAs. Numbers below the bar indicates normalized log10 values of read counts. (B) Dual-luciferase reporter assays using HEK293T cells co-transfected with miRNA mimics and recombinant pmirGLO vectors containing the predicted binding sites of miR-296, miR-423, let-7 and miR-278 in the CDS of *Kr-h1*. *, $P < 0.05$ and **, $P < 0.01$ compared to the negative control of mimics (mimics-ck). n = 6. (C) Dual-luciferase reporter assays using HEK293T cells co-transfected with miRNA mimics and recombinant pmirGLO vectors containing the predicted binding

sites of miR-14, miR-998 and miR-2765 in the 3'UTR of *Kr-h1*. n.s., no significant difference. n = 6. (D, E) Dual-luciferase reporter assays using HEK293T cells co-transfected with let-7 mimics (D) or miR-278 mimics (E) plus recombinant pmirGLO vectors containing either wildtype (WT) or mutated (MT) binding sites of let-7 or miR-278. **, $P < 0.01$ and ***, $P < 0.001$ compared to the negative control of mimics (mimics-ck). n = 6.

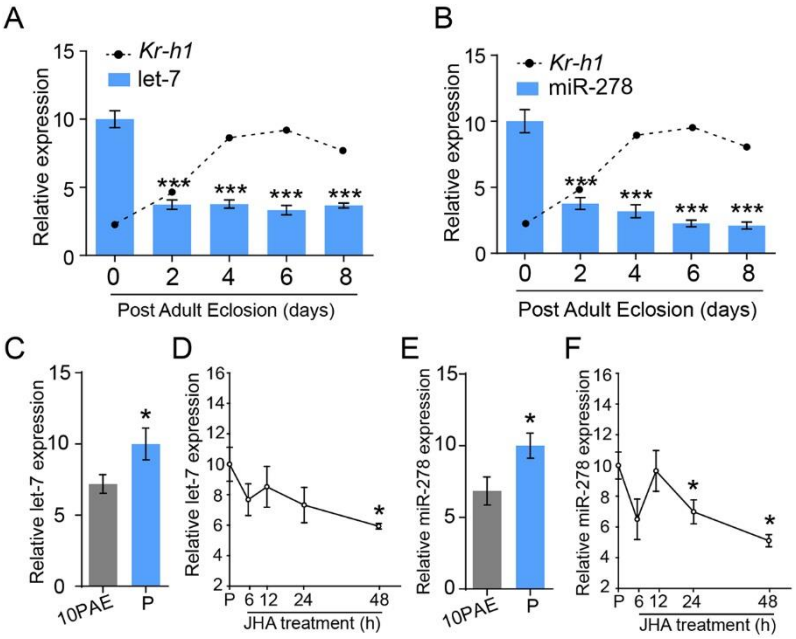

Fig. 2. Temporal expression patterns of let-7 and miR-278 and their responsiveness to JH. (A, B) Developmental profiles of let-7 (A) and miR-278 (B) in the fat body of adult females collected at 0, 2, 4, 6 and 8 days post adult eclosion. The dashed lines indicate the expression pattern of *Kr-h1*, as a parallel comparison. ***, $P < 0.001$ compared to that on the day of adult eclosion (day 0). n = 8. (C-F) The relative levels of let-7 (C and D) and miR-278 (E and F) expression in the fat body of adult females collected at 10 days post adult eclosion (10PAE) as well as those treated with ethoxyprecocene (P) for 10 days and further treated with methoprene (JHA) for 6-48 h. *, $P < 0.05$ compared to 10PAE (C and E) (n = 14) or compared to P (D and F) (n = 8).

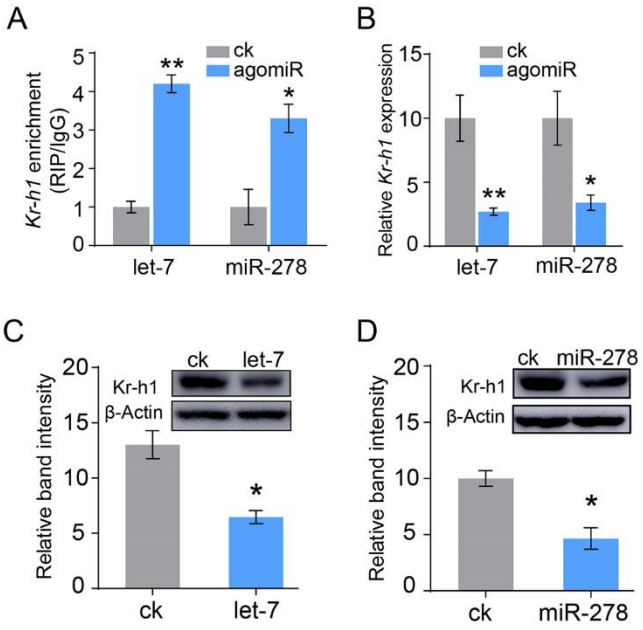

Fig. 3. let-7 and miR-278 bind *Kr-h1* mRNA and downregulate its expression *in vivo*. (A) RNA immunoprecipitation (RIP) showing the relative abundance of precipitated *Kr-h1* mRNA in the fat body of adult females injected with let-7 and miR-278 agomiRs. *, $P < 0.05$ and **, $P < 0.01$ compared to the negative controls (ck). n = 4. (B) qRT-PCR showing the effect of let-7 and miR-278 agomiR treatment on *Kr-h1* mRNA levels in the fat body of adult females. *, $P < 0.05$ and **, $P < 0.01$ compared to the negative controls (ck). n = 10. (C, D) Western blot and subsequent quantification of band intensity showing the effect of let-7 (C) and miR-278 (D) agomiR treatment on Kr-h1 protein levels in the fat body of adult females. *, $P < 0.05$ compared to the negative controls (ck). n = 3.

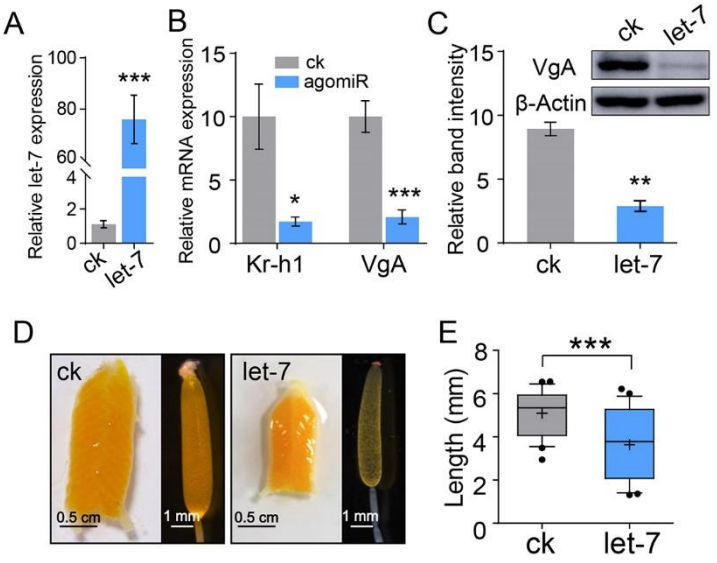

Fig. 4. Effect of let-7 agomiR treatment on locust vitellogenesis, oocyte maturation and ovarian growth. (A) Relative abundance of let-7 in the fat body of adult females injected with let-7 agomiR vs. the negative control (ck). ***, $P < 0.001$ compared to the negative control (ck). n =10-12. (B) Relative levels of *Kr-h1* and *VgA* mRNAs in the fat body of adult females injected with let-7 agomiR vs. the negative control (ck). *, $P < 0.05$ and ***, $P < 0.001$. n = 12. (C) Western blot and quantification of band intensity showing the decrease of VgA protein levels after let-7 agomiR treatment. **, $P < 0.01$ compared to the negative control (ck). n = 3. (D) Representative phenotypes of ovaries and primary oocytes after let-7 agomiR treatment vs. the negative control (ck). Scale bars: ovary, 0.5 cm; primary oocyte, 1 mm. (E) Statistical analysis of primary oocyte lengths between the groups of let-7 agomiR treatment and the negative control (ck). ***, $P < 0.001$. n = 12.

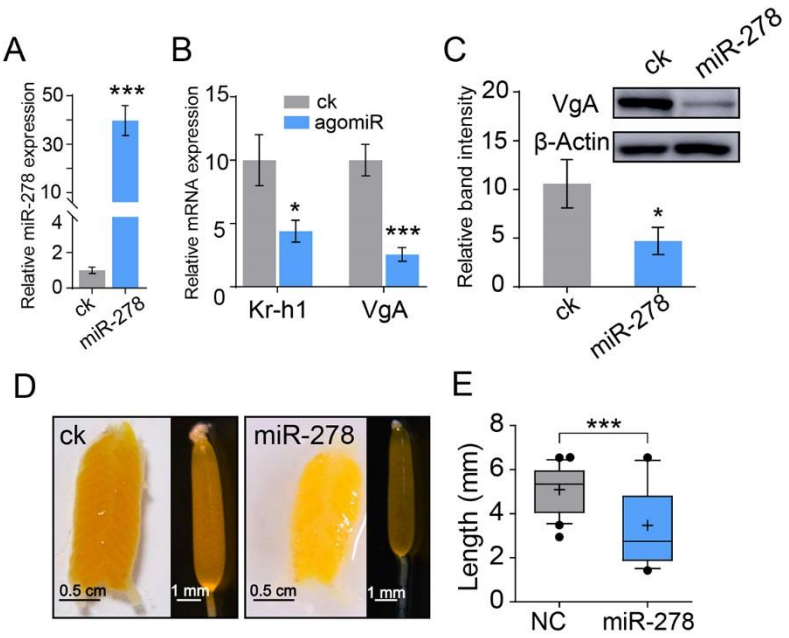

Fig. 5. Effect of miR-278 agomiR treatment on locust vitellogenesis, oocyte maturation and ovarian growth. (A) Relative abundance of miR-278 in the fat body of adult females injected with miR-278 agomiR vs. the negative control (ck). ***, $P < 0.001$. n = 12. (B) Relative levels of *Kr-h1* and *VgA* mRNAs in the fat body of adult females injected with miR-278 agomiR vs. the negative control (ck). *, $P < 0.05$ and ***, $P < 0.001$. n = 12. (C) Western blot and quantification of band intensity showing the decrease of VgA protein levels after miR-278 agomiR treatment. *, $P < 0.05$ compared to the negative control (ck). n = 3. (D) Representative phenotypes of ovaries and primary oocytes after miR-278 agomiR treatment vs. the negative control (ck). Scale bars: ovary, 0.5 cm; ovariole, 1 mm. (E) Statistical analysis of primary oocyte lengths between the groups of miR-278 agomiR treatment and the negative control (ck). ***, $P < 0.001$. n = 12.

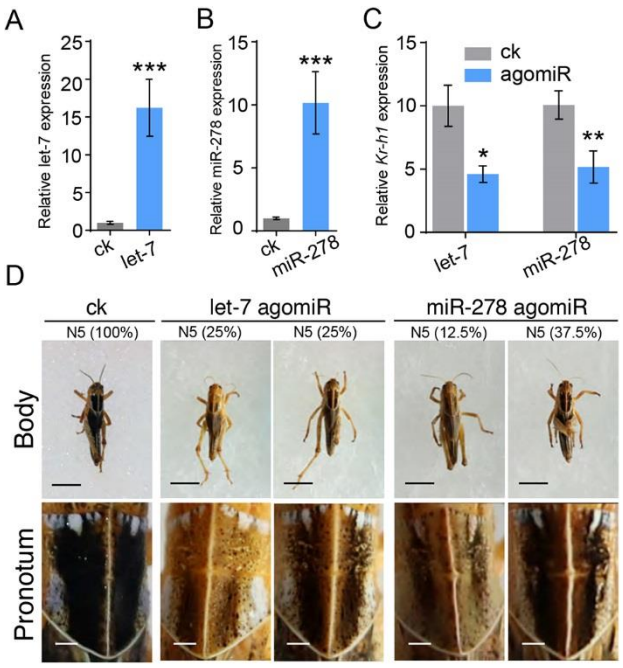

Fig. 6. Effect of let-7 and miR-278 agomiR treatment on locust metamorphosis. (A, B) The abundance of let-7 (A) and miR-278 (B) in the whole body of final 5th instar nymphs previously subjected to the respective agomiR treatment at the penultimate 4th nymphal instar. ***, $P < 0.001$ compared to the negative controls (ck). n = 16. (C) Effect of let-7 and miR-278 agomiR treatment on *Kr-h1* expression in the nymphs. agomiRs were injected at the penultimate 4th nymphal instar, and *Kr-h1* mRNA levels were measured in the whole body at the final 5th nymphal instar. *, $P < 0.05$ and **, $P < 0.01$ compared to the negative controls (ck). n = 26. (D) The representative phenotypes and percentage of partially precocious metamorphosis at the final 5th nymphal instar (N5), previously treated with let-7 and miR-278 agomiRs at the penultimate 4th nymphal instar (3 replicates with 16 locusts in each treatment). Upper panel, whole body (scale bar, 1 cm). Lower panel, enlarged images of the pronotum (scale bar, 0.1 cm). ck, the negative control.

Supplementary information

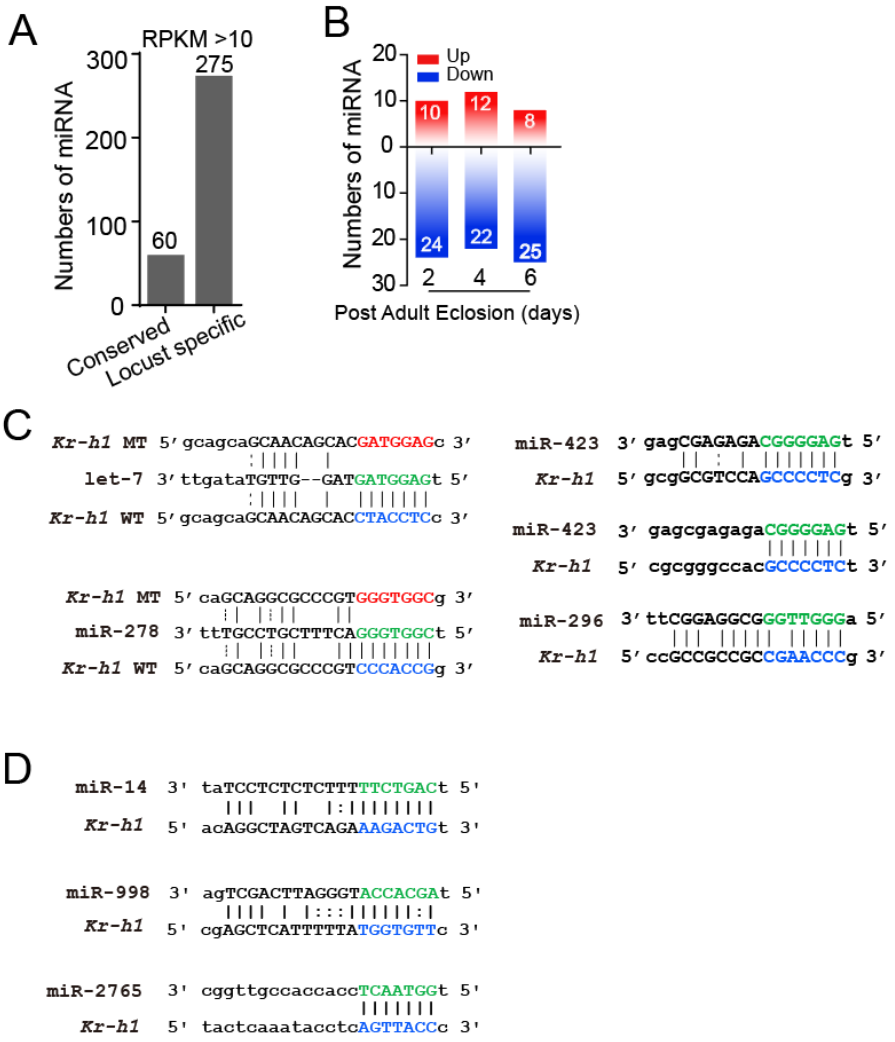

Fig. S1. **miRNA identification and binding site prediction for *Kr-h1*.** (A) Numbers of conserved miRNA and locust specific miRNA with RPKM values > 10. (B) The number of upregulated and downregulated miRNAs in the fat body of adult females at 2, 4 and 6 days post adult eclosion compared to that on the day of adult eclosion. (C, D) Sequence alignment of miRNAs with their predicted binding sites in the CDS (C) and 3′UTR (D) of *Kr-h1*. The binding sites (blue) in *Kr-h1* complementary to the seed region (green) of let-7 and miR-278 were site-mutated to their complementary bases (red) in the luciferase reporter assays.

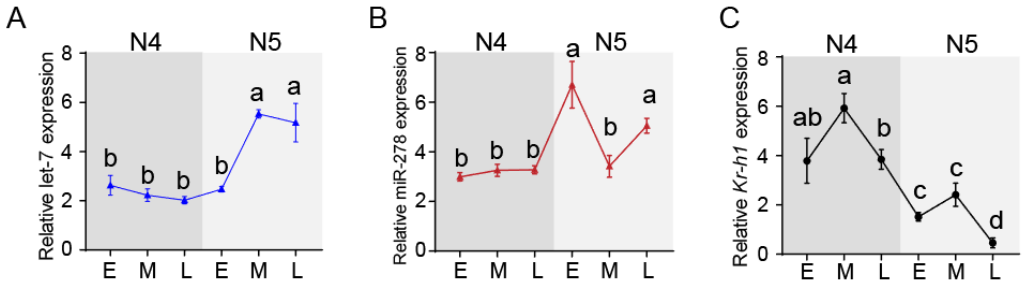

Fig. S2. The temporal expression patterns of let-7, miR-278 and *Kr-h1* in late-instar locust nymphs. qRT-PCR showing the relative levels of let-7 (A), miR-278 (B) and *Kr-h1* (C) expression in the whole body of penultimate 4th (N4) and final 5th (N5) instar nymphs. E, M, and L indicate the early (day 1), middle (day 2 for N4, and day 3 for N5), and late (day 4 for N4, and day 5 for N5) stages, respectively. The duration of 4th and 5th instar nymphs was about 4 days and 5 days, respectively under our reading conditions. In each panel, the means labeled with different letters indicate significant difference at $P < 0.05$. n = 8.

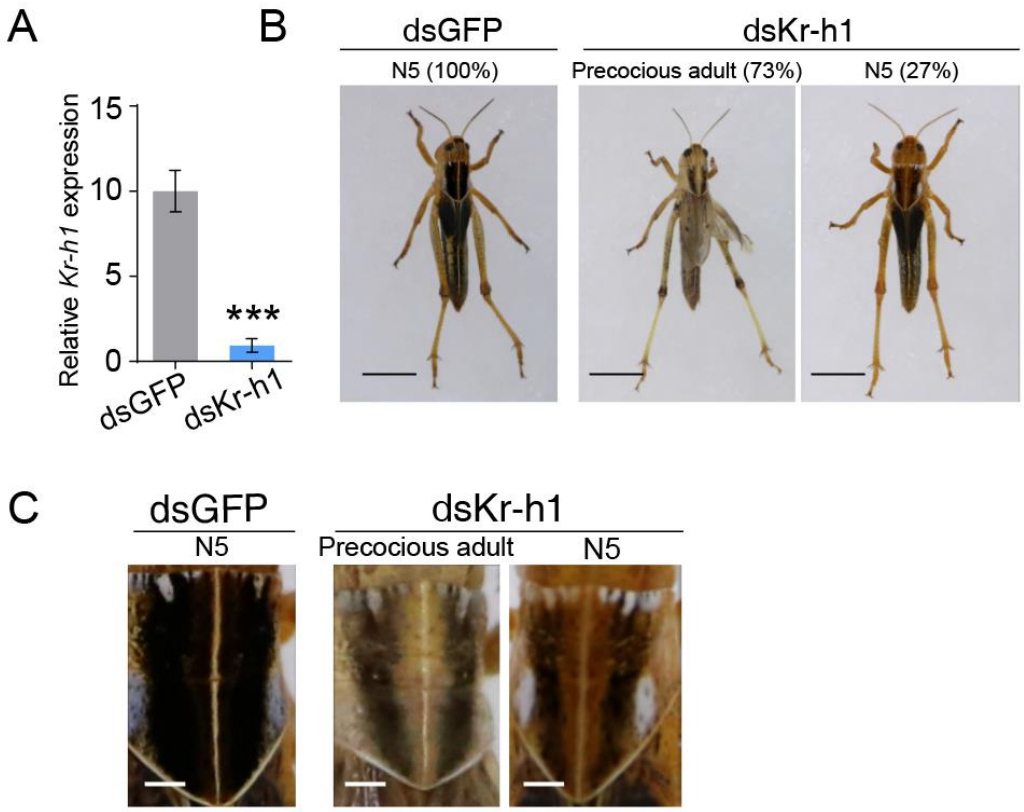

Fig. S3. Effect of *Kr-h1* knockdown on locust metamorphosis. (A) RNAi-mediated knockdown efficiency of *Kr-h1* in the whole body of final 5th instar nymphs previously subjected to dsKr-h1 treatment at the penultimate 4th nymphal instar. ***, $P < 0.001$ compared to the dsGFP control. n = 7-8. (B) Representative phenotypes and percentage of precocious metamorphosis at the final instar nymphs (N5) previously subjected to dsKr-h1 treatment at the penultimate 4th nymph instar (3 replicates with 7-8 locusts in each treatment). Scale bar, 1 cm. (C) Enlarged images of the pronotum shown in (B). Scale bar, 0.1 cm.

Table S1. Primers used in qRT-PCR, mutation and RNAi.

Primer Name	Sequence (5' to 3')
qRT-PCR	
qKr-h1-F	ACTTCGTCTTCTGGAATGA
qKr-h1-R	GGCAATCGGTATTACACTTAG
qlet-7-F	GCTGAGGTAGTAGGTTGTATAGTT
qmiR-278-F	GGTGGGACTTTCGTCCGTTT
qU6	ACACTCCAGCTGGGTCAAAATCGTGAAGCG
qVgA-F	CCCACAAGAAGCACAGAACG
qVgA-R	TTGGTCGCCATCAACAGAAG
qActin-F	AATTACCATTGGTAACGAGCGATT
qActin-R	TGCTTCCATACCCAGGAATGA
site mutation	
mut-let-7-F	CCTCTGCTTGATGATGGAGTACTCGCAGCAGGCGCCCGTCCCAC
mut-let-7-R	CGAGTACTCCATCATCAAGCAGAGGTCGCGACCGCCCCCGGGCGT
mut-miR-278-F	GCGCCCGTTGATGACGCGCACGCGGGCCACGCCCCTCTCTCC
mut-miR-278-R	CGTGCGCGTCATCAACGGGCGCCTGCTGCGAGTACAGGTAGT
dsRNA synthesis	
dsKr-h1-F	GTCAAGGAGAACCTGAGCGTGC
dsKr-h1-R	TGCTGCTGCTCCGAGTGGCT
dsGFP-F	CACAAGTTCAGCGTGTCCG
dsGFP-R	GTTCACCTTGATGCCGTTC

Supplementary information

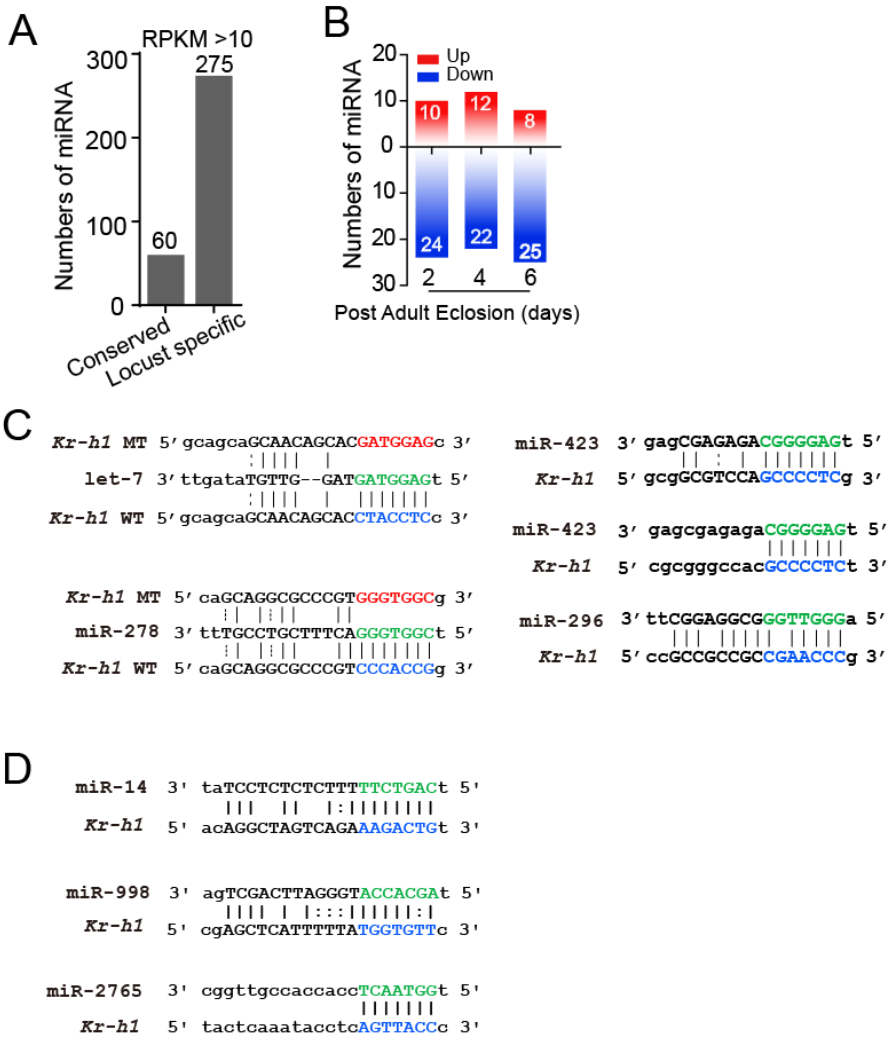

Fig. S1. **miRNA identification and binding site prediction for *Kr-h1*.** (A) Numbers of conserved miRNA and locust specific miRNA with RPKM values > 10. (B) The number of upregulated and downregulated miRNAs in the fat body of adult females at 2, 4 and 6 days post adult eclosion compared to that on the day of adult eclosion. (C, D) Sequence alignment of miRNAs with their predicted binding sites in the CDS (C) and 3′UTR (D) of *Kr-h1*. The binding sites (blue) in *Kr-h1* complementary to the seed region (green) of let-7 and miR-278 were site-mutated to their complementary bases (red) in the luciferase reporter assays.

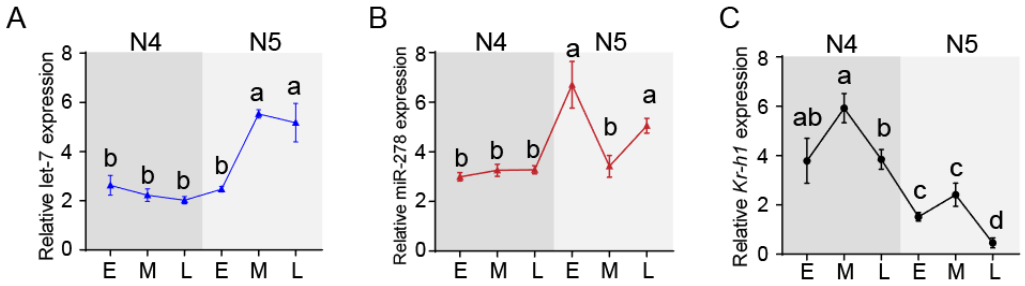

Fig. S2. The temporal expression patterns of let-7, miR-278 and *Kr-h1* in late-instar locust nymphs. qRT-PCR showing the relative levels of let-7 (A), miR-278 (B) and *Kr-h1* (C) expression in the whole body of penultimate 4th (N4) and final 5th (N5) instar nymphs. E, M, and L indicate the early (day 1), middle (day 2 for N4, and day 3 for N5), and late (day 4 for N4, and day 5 for N5) stages, respectively. The duration of 4th and 5th instar nymphs was about 4 days and 5 days, respectively under our reading conditions. In each panel, the means labeled with different letters indicate significant difference at $P < 0.05$. n = 8.

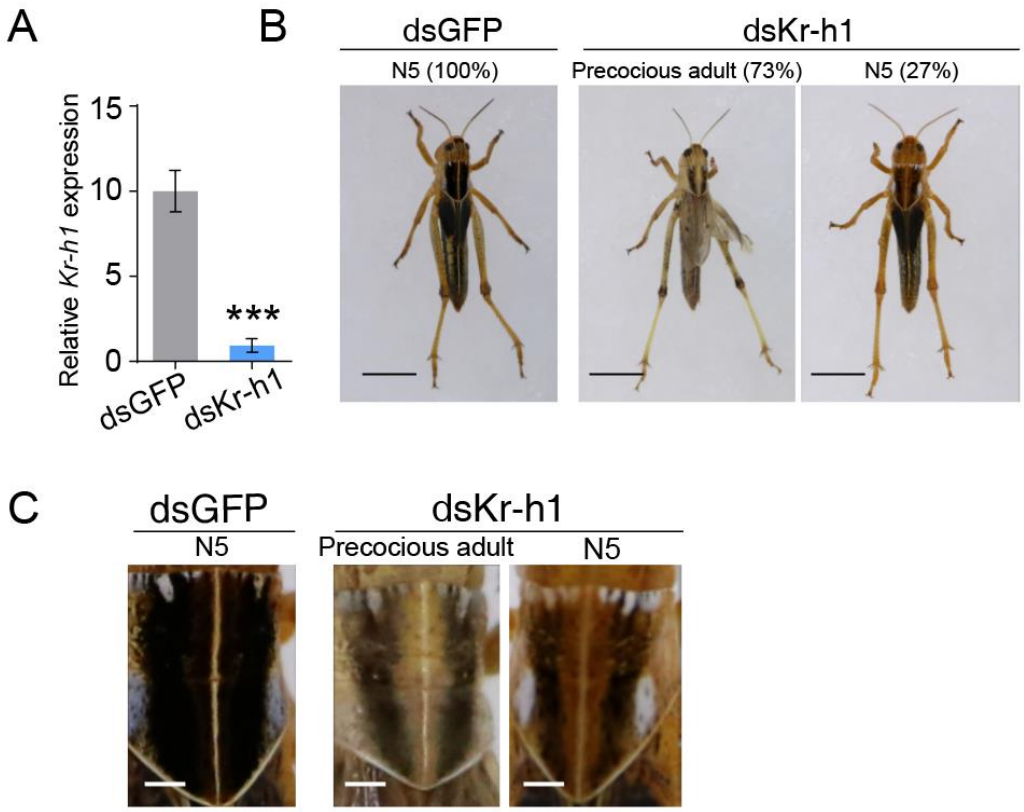

Fig. S3. Effect of *Kr-h1* knockdown on locust metamorphosis. (A) RNAi-mediated knockdown efficiency of *Kr-h1* in the whole body of final 5th instar nymphs previously subjected to dsKr-h1 treatment at the penultimate 4th nymphal instar. ***, $P < 0.001$ compared to the dsGFP control. n = 7-8. (B) Representative phenotypes and percentage of precocious metamorphosis at the final instar nymphs (N5) previously subjected to dsKr-h1 treatment at the penultimate 4th nymph instar (3 replicates with 7-8 locusts in each treatment). Scale bar, 1 cm. (C) Enlarged images of the pronotum shown in (B). Scale bar, 0.1 cm.

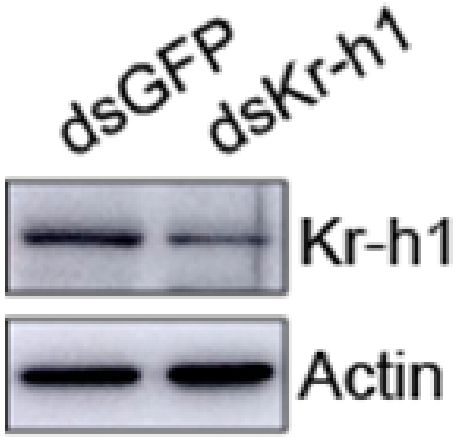

Fig. S4. Specificity of the antiserum. The antiserum specificity was verified by western blot using protein extracted from fat body of locusts treated with dsKr-h1 versus dsGFP.

Table S1. Primers used in qRT-PCR, mutation and RNAi.

Primer Name	Sequence (5' to 3')
qRT-PCR	
qKr-h1-F	ACTTCGTCTTCTGGAATGA
qKr-h1-R	GGCAATCGGTATTACACTTAG
qlet-7-F	GCTGAGGTAGTAGGTTGTATAGTT
qmiR-278-F	GGTGGGACTTTCGTCCGTTT
qU6	ACACTCCAGCTGGGTCAAAATCGTGAAGCG
qVgA-F	CCCACAAGAAGCACAGAACG
qVgA-R	TTGGTCGCCATCAACAGAAG
qActin-F	AATTACCATTGGTAACGAGCGATT
qActin-R	TGCTTCCATACCCAGGAATGA
site mutation	
mut-let-7-F	CCTCTGCTTGATGATGGAGTACTCGCAGCAGGCGCCCGTCCCAC
mut-let-7-R	CGAGTACTCCATCATCAAGCAGAGGTCGCGACCGCCCCCGGGCGT
mut-miR-278-F	GCGCCCGTTGATGACGCGCACGCGGGCCACGCCCCTCTCTCC
mut-miR-278-R	CGTGCGCGTCATCAACGGGCGCCTGCTGCGAGTACAGGTAGT
dsRNA synthesis	
dsKr-h1-F	GTCAAGGAGAACCTGAGCGTGC
dsKr-h1-R	TGCTGCTGCTCCGAGTGGCT
dsGFP-F	CACAAGTTCAGCGTGTCCG
dsGFP-R	GTTCACCTTGATGCCGTTC